

DUAL-WAVELENGTH FLUORESCENCE STUDY OF *IN VIVO* ACCUMULATION AND FORMATION OF 5-ALA-INDUCED PORPHYRINS

Zavedeeva V.E.¹, Efendiev K.T.^{2,3}, Kustov D.M.², Loschenova L.Yu.⁴, Loschenov V.B.^{2,3}

¹Sorbonne University, Faculty of Science and Engineering, Paris, France

²Prokhorov General Physics Institute of the Russian Academy of Sciences, Moscow, Russia

³National Research Nuclear University «MEPhI», Moscow, Russia

⁴BIOSPEC Ltd., Moscow, Russia

Abstract

This article discusses the processes of 5-aminolevulinic acid (5-ALA) metabolism, as well as the accumulation and photobleaching of protoporphyrin IX (PpIX) during photodynamic therapy (PDT) of benign skin tumors using the application method of introducing a 20% 5-ALA solution. The exposure time of the drug was 4 h. The study included two patients, one with dermatofibroma and one with congenital melanocytic nevus. Spectral fluorescence study was performed by fluorescence excitation using lasers at wavelengths of 405 and 632.8 nm. Fluorescence of normal and pathological tissues was recorded in the range of 350–800 nm at $\lambda_{exc}=405$ nm and in the range of 600–750 nm at $\lambda_{exc}=632.8$ nm. The dynamics of PpIX accumulation was studied. In the superficial tissue layers (at $\lambda_{exc}=405$ nm), the maximum accumulation of PpIX was recorded 3 h after the 5-ALA administration. In deeper tissue layers (at $\lambda_{exc}=632.8$ nm), the PpIX accumulation increased during 4 h of observation. After PDT with laser radiation with a wavelength of 635 nm, photobleaching of PpIX and the formation of its chlorin-type photoproducts with a fluorescence maximum in the range of 670–700 nm were observed. It was not possible to establish the presence of uroporphyrins I and III and/or coproporphyrin I, which could indicate a disturbance in the mitochondrial metabolism of necrotic cells. The obtained results expand the possibilities of spectral-fluorescent diagnostics and can contribute to increasing the effectiveness of 5-ALA-PDT of tumors.

Key words: spectral fluorescence diagnostics, photodynamic therapy, 5-aminolevulinic acid, porphyrins, protoporphyrin IX, chlorin-type photoproducts, fluorescence spectra.

Contacts: Zavedeeva V.E., e-mail: vezavedeeva@gmail.com

For citations: Zavedeeva V.E., Efendiev K.T., Kustov D.M., Loschenova L.Yu., Loschenov V.B. Dual-wavelength fluorescence study of *in vivo* accumulation and formation of 5-ALA-induced porphyrins, *Biomedical Photonics*, 2025, vol. 14, no. 1, pp. 36–46. doi: 10.24931/2413–9432–2025–14–1–36–46

ДВУХВОЛНОВОЕ ФЛУОРЕСЦЕНТНОЕ ИССЛЕДОВАНИЕ *IN VIVO* НАКОПЛЕНИЯ И ОБРАЗОВАНИЯ 5-АЛК-ИНДУЦИРОВАННЫХ ПОРФИРИНОВ

В.Е. Заведеева¹, К.Т. Эфендиев^{2,3}, Д.М. Кустов², Л.Ю. Лощенова⁴, В.Б. Лощенов^{2,3}

¹Университет Сорбонна, Факультет науки и инженерии, Париж, Франция

²Институт общей физики им. А.М. Прохорова РАН, Москва, Россия

³Национальный исследовательский ядерный университет «МИФИ», Москва, Россия

⁴ООО «БИОСПЕК», Москва, Россия

Резюме

В данной статье рассмотрены процессы метаболизма 5-аминолевулиновой кислоты (5-АЛК), а также накопления и фотообесцвечивания протопорфирина IX (ПпIX) в процессе фотодинамической терапии (ФДТ) доброкачественных опухолей кожи с применением аппликационного способа введения 20%-го раствора 5-АЛК. Время экспозиции препарата составило 4 ч. В исследовании участвовали два пациента с дерматофибромой и врожденным меланоцитарным невусом. Спектрально-флуоресцентное исследование проводили с возбуждением флуоресценции лазерами на длинах волн 405 и 632,8 нм. Флуоресценцию нормальной и патологически измененной ткани регистрировали в диапазоне 350–800 нм при $\lambda_{exc}=405$ нм и в диапазоне 600–750 нм при $\lambda_{exc}=632,8$ нм. Исследована динамика накопления ПпIX. В поверхностных слоях тканей (при $\lambda_{exc}=405$ нм) максимум накопления ПпIX регистрировали спустя 3 ч после введения 5-АЛК. В более глубоких слоях тканей (при $\lambda_{exc}=632,8$ нм) накопление ПпIX увеличивалось в течение 4 ч наблюдения. После ФДТ

лазерным излучением с длиной волны 635 нм наблюдали фотообесцвечивание ПпIX и образование его фотопродуктов хлоринового типа, с максимумом флуоресценции в диапазоне 670–700 нм. Установить наличие уропорфиринов I и III и/или копропорфирина I, которые могли бы свидетельствовать о нарушении митохондриального метаболизма некротических клеток, не удалось. Полученные результаты расширяют возможности спектрально-флуоресцентной диагностики и могут способствовать повышению эффективности 5-АЛК-ФДТ опухоли.

Ключевые слова: спектрально-флуоресцентная диагностика, фотодинамическая терапия, 5-аминолевулиновая кислота, порфирины, протопорфирин IX, фотопродукты хлоринового типа, спектры флуоресценции.

Контакты: Заведеева В.Е., e-mail: vezavedeeva@gmail.com

Для цитирования: Заведеева В.Е., Эфендиев К.Т., Кустов Д.М., Лощенова Л.Ю., Лощенов В.Б. Двухволновое флуоресцентное исследование *in vivo* накопления и образования 5-алк-индуцированных порфиринов // Biomedical Photonics. – 2025. – Т. 14, № 1. – С. 36–46. doi: 10.24931/2413–9432–2025–14–1–36–46

Introduction

Fluorescence diagnostics and photodynamic therapy (PDT) using 5-aminolevulinic acid (5-ALA) are widely used in leading clinics around the world to treat various oncological and non-oncological diseases. PDT includes two key steps: administration of a photosensitizer (PS) which has the ability to selectively accumulate in tumor tissues and cells, and then exposure of the sensitized tissues to light of a specific wavelength. It is optimal if the wavelength corresponds to one of the PS absorption peaks, which triggers the process of generation of reactive oxygen species, mainly singlet oxygen (Fig. 1).

The transfer of molecular oxygen from the triplet state to the singlet state is facilitated by the energy transfer from the PS in the excited triplet state. When the PS absorbs laser radiation, the molecule passes into an excited state, which can exist in either singlet or triplet configuration. The PS molecule in the singlet state quickly passes back to the ground state, accompanied by the emission of light quanta (fluorescence) or is converted into kinetic thermal energy

of the reaction products. In contrast, the PS in the triplet state has a longer lifetime, which increases the probability of energy transfer to nearby (within 0–20 nm) oxygen molecules, thereby transferring them to the singlet state. According to [1], 5-ALA has two metabolic pathways. The first pathway leads to the formation of photodynamically active protoporphyrin IX (PpIX). The second pathway leads to the formation of fluorescent uroporphyrin I, which either does not have photodynamic activity or exhibits it to an insignificant degree (Fig. 2).

It is especially important that 5-ALA metabolism in necrotic tissues has been shown to occur via an alternative pathway [1]. In cells that have undergone apoptosis under the influence of PDT, metabolic disturbances are also observed, which indicates the possibility of switching the metabolism of irradiated cells to an alternative pathway. Furthermore, it has been demonstrated that the intensity of the PpIX accumulation process diminishes with laser irradiation when light exposure occurs prior to reaching maximum accumulation [1]. This phenomenon can likely

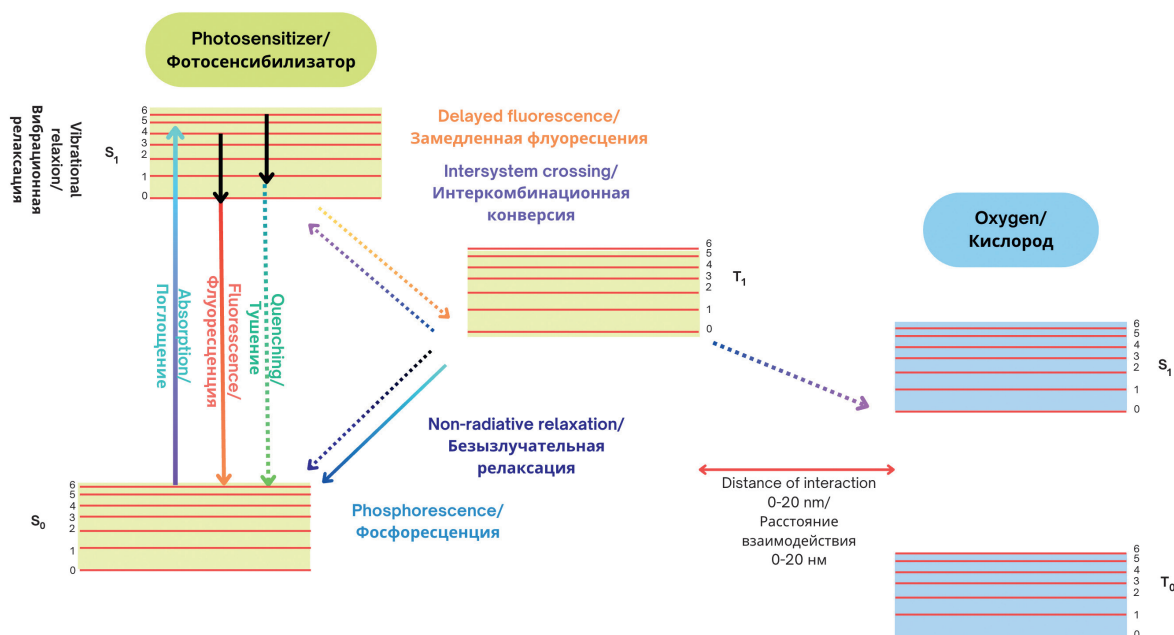


Рис. 1. Схема образования возбужденного (синглетного) состояния кислорода в процессе ФДТ.

Fig. 1. Scheme of formation of the excited (singlet) oxygen state in the PDT process.

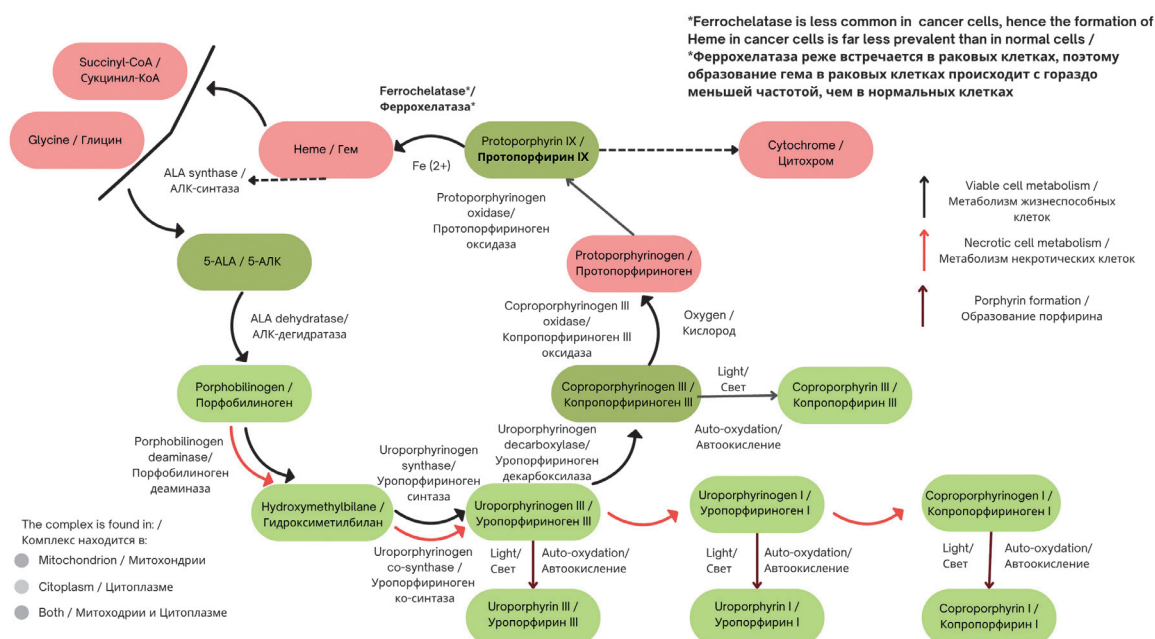


Рис. 2. Схема метаболических путей 5-АЛК в нормальных, раковых и некротических клетках.
Fig. 2. Scheme of metabolic pathways in normal, cancerous and necrotic cells.

be attributed to the requirement of molecular oxygen for the conversion of coproporphyrinogen III to PpIX. It can be hypothesized that premature irradiation limits the access of molecular oxygen to coproporphyrinogen III, since it leads to the activation of molecular oxygen to its singlet state, which, in turn, prevents the formation of PpIX.

Therefore, two competing mechanisms can be identified: one that reduces photodynamic activity and the other one that increases it. The isolation of the spectra of the products of natural metabolism of 5-ALA and its photochemical transformation *in vivo* is a methodologically complex process. This complexity arises from the substantial overlap between the absorption and fluorescence spectra of these compounds. The current state of technical capabilities precludes the simultaneous excitation of several wavelengths corresponding to the

absorption of various porphyrin derivatives of 5-ALA, as well as the effective separation of the recorded spectra.

In order to solve this problem, it is necessary to have precise knowledge of the absorption and fluorescence spectra of the porphyrins under study in the biological tissues under study. In this case, the focus is on porphyrins such as uroporphyrin I, uroporphyrin III, coproporphyrin I, coproporphyrin III and PpIX. However, the spectra of these fluorophores are most often reported for acidic, alkaline, or other media that do not correspond to the physiological conditions of the human body. Fig. 3–4 illustrate the absorption and fluorescence spectra of uroporphyrins I and III, coproporphyrin I, and PpIX in various media [2, 3].

Table 1 shows the characteristic fluorescence and absorption maxima of coproporphyrin I, uroporphyrin I, uroporphyrin III and PpIX [2, 3].

Таблица 1.
Сравнительная таблица пиков флуоресценции и поглощения копропорфирина I, уропорфирина I, уропорфирина III и ПпIX [2,3]

Table 1.
Comparative table of fluorescence and absorption peaks of coproporphyrin I, uroporphyrin I, uroporphyrin III and PpX [2,3]

Porphyrin Порфирин	Максимум поглощения, нм Absorption maximum, nm					Максимум флуоресценции, нм Fluorescence maximum, nm		
	1	2	3	4	5	1	2	3
КР I CP I	375	389	503	537	559	609	614	677
УП I UP I	406	552	592	-	-	-	-	-
УП III UP III	398	502	538	560	612	-	618	681
Пп IX Pp IX	408	506	542	577	631	-	633	722

КП I – копропорфирин I, УП I – уропорфирин I, УП III – уропорфирин III, Пп IX – протопорфирин IX
CP I – coproporphyrin I, UP I – uroporphyrin I, UP III – uroporphyrin III, Pp IX – protoporphyrin IX

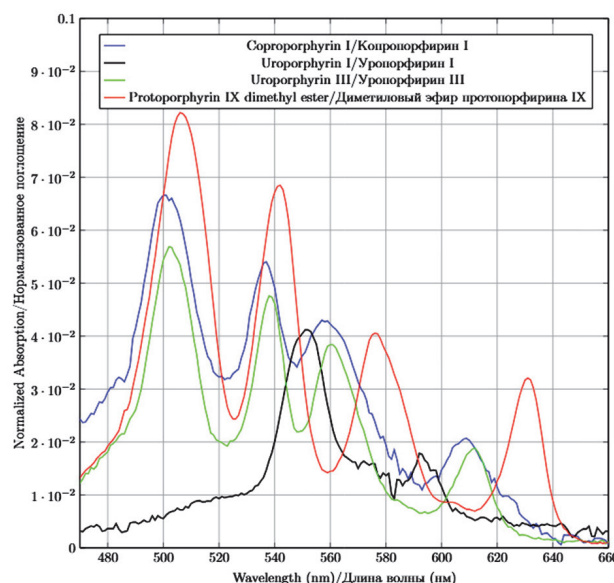
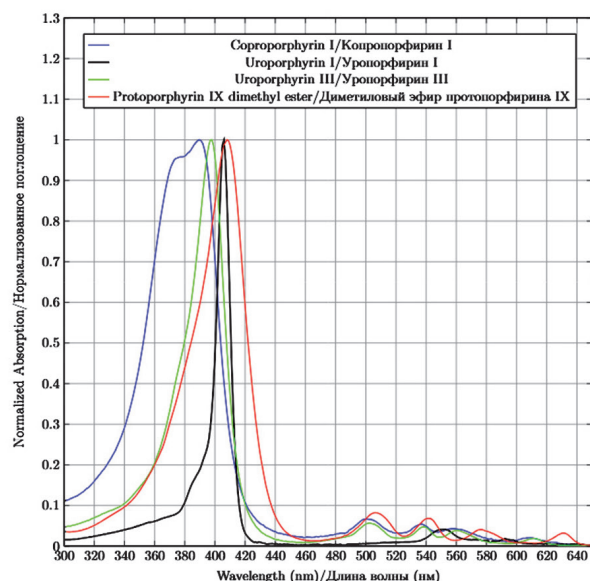


Рис. 3. Спектры поглощения 5-АЛК-индуцированных порфиринов: раствора КП I в 0,1 М калийно-фосфатного буфера, раствора УП I в 1,0 М растворе соляной кислоты, раствора УП III в 0,1 М растворе калийно-фосфатного буфера и раствора ПпIX диметил эстера в хлороформе [2, 3].

Fig. 3. Absorption spectra of 5-ALA-induced porphyrins: a solution of coproporphyrin I in 0.1 M potassium phosphate buffer, a solution of uroporphyrin I in 1.0 M hydrochloric acid, a solution of uroporphyrin III in 0.1 M potassium phosphate buffer, and a solution of PpIX dimethyl ester in chloroform [2, 3].

The purpose of this study is to characterize the absorption and fluorescence spectra of 5-ALA-induced porphyrins for subsequent use in spectral separation. In addition, to investigate the formation of PpIX photoproducts - chemical compounds formed as a result of photochemical reactions during PDT.

Differences in the fluorescence lifetime of uroporphyrin I, coproporphyrin III, PpIX and its photoproducts open up the possibility of differentiating the metabolic pathways of 5-ALA. From a practical point of view, this is especially important, since such differentiation of spectra can allow the presence of necrotic tissue in the irradiated area to be detected even before the start of PDT.

Monitoring of PpIX concentration and its photobleaching in different parts of the irradiated tissue is of greatest interest, as it can help to detect initiated processes of necrotic or apoptotic cell death. If in certain parts of the tissue the concentration of PpIX is lower than in the actively proliferating part of the tumor, and the fluorescence intensity does not decrease after irradiation, it may indicate partial necrotization of the tissue or lack of oxygen access caused by stenosis or obstruction of blood vessels.

Materials and methods

Patients

This study included two clinical cases of benign skin tumors – dermatofibroma and congenital melanocytic nevus. Both patients underwent spectral fluorescence diagnostics to assess the accumulation of 5-ALA-induced porphyrins before and after PDT. The dynamics of accumulation and the intensity of photobleaching of PpIX in different tissue layers were also studied. The main parameters of the patients involved in the study are presented in Table 2.

Fig. 5 shows images of patients' tumors with indication of the areas where spectral fluorescence diagnostics was performed.

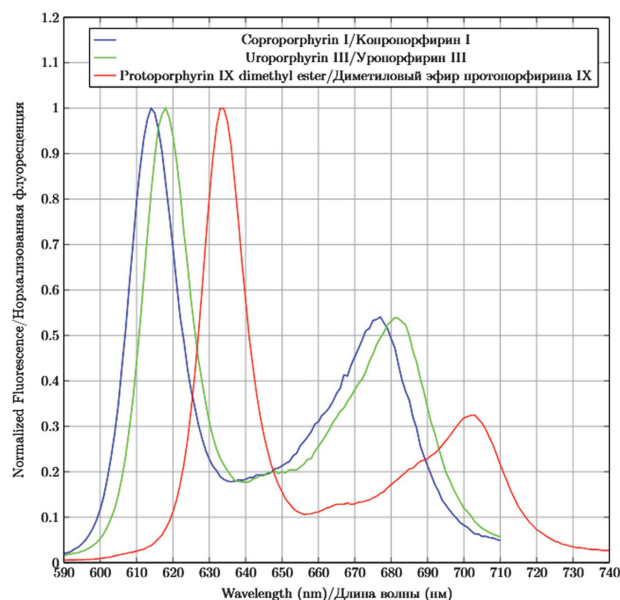
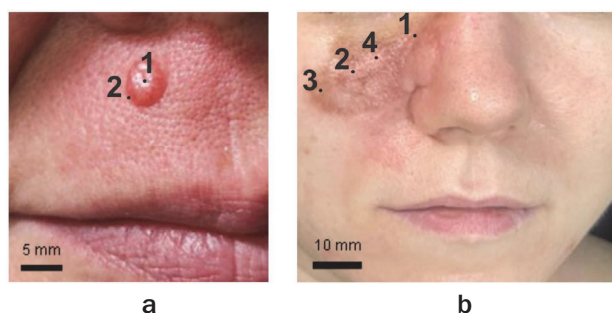


Рис. 4. Спектры флуоресценции 5-АЛК индуцированных порфиринов: раствора КП I в 0,1 М калийно-фосфатного буфера, раствора УП III в 0,1 М калийно-фосфатного буфера и раствора ПпIX диметил эстера в растворе метанола [2, 3].

Fig. 4. Fluorescence spectra of 5-ALA-induced porphyrins: a solution of coproporphyrin I in 0.1 M potassium phosphate buffer, a solution of uroporphyrin III in 0.1 M potassium phosphate buffer, and a solution of PpIX dimethyl ester in methanol solution [2, 3].

Таблица 2
Основные параметры пациентов**Table 2**
Main parameters of patients

Параметр Parameter	Пациент 1 Patient 1	Пациент 2 Patient 2
Диагноз Diagnosis	Дерматофиброма Dermatofibroma	Врожденный меланоцитарный невус Congenital melanocytic nevus
Пол Gender	женский female	женский female
Возраст Age	56 лет 56 years	35 лет 35 years

**Рис. 5.** Опухоли с указанием зон, где проводили флуоресцентные исследования: а – пациент с дерматофибромой (зона 1 – центральная область опухоли; зона 2 – периферия опухоли); б – пациент с врожденным меланоцитарным невусом (зоны 1–3 – области с повышенным содержанием меланоцитов; зона 4 – область свободная от меланоцитов).**Fig. 5.** Tumors with indication of the zones where fluorescence studies were performed: a – patient with dermatofibroma (zone 1 – central area of the tumor; zone 2 – tumor periphery); b – patient with congenital melanocytic nevus (zones 1–3 – areas with increased content of melanocytes; zone 4 – area free of melanocytes).

The study included several stages, one of them being spectral-fluorescent studies of the accumulation and photobleaching of PpIX (Fig. 6).

For 24 h after the administration of 5-ALA, patients strictly observed the light regime (excluding exposure to direct sunlight, watching television programs, etc.). All procedures were carried out in accordance with the recommendations of the Helsinki Declaration of the World Medical Association.

Photosensitizer

A 20% aqueous solution of 5-ALA prepared immediately before use was utilized for the spectral-fluorescent study. The administration was carried out by the application method: a sterile gauze napkin was soaked in the solution and applied to the area of the pathological focus. Before applying the preparation, the skin was cleaned with distilled water.

To prevent evaporation of the 5-ALA solution and improve its penetration, the treated area was covered with cling film. During the entire observation period of 5-ALA-induced PpIX accumulation (up to 4 h), the patient was in a darkened room to minimize exposure to external light.

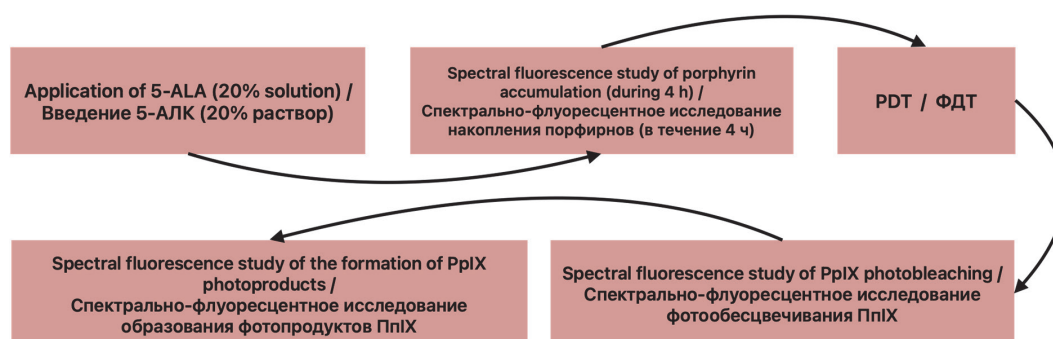
Spectral fluorescence diagnostics

Laser electron-spectral unit LESA-01-BIOSPEC (BIOSPEC Ltd., Moscow) was used for spectral-fluorescence study. Tissue fluorescence was excited by laser irradiation with wavelengths of 405 and 632.8 nm. Excitation with wavelength in blue and red spectral bands was performed in order to study the distribution of PpIX in superficial and deeper tissue layers [4]. When the fluorescence was excited at 405 nm wavelength, the spectral signal was recorded in the range of 350–800 nm. While excited at 632.8 nm wavelength, the spectral signal was recorded in the range of 600–750 nm, respectively. Both bands included diffusely scattered laser emission signal and tissue fluorescence in the red region of the spectrum.

Spectral fluorescence imaging of normal skin and neoplasm skin was performed before PS injection to determine endogenous tissue fluorescence. The cheek skin was chosen as a reference in measurements. Tissue fluorescence spectra were also recorded 1, 2, 3, and 4 hours after 5-ALA application, before the start of PDT. Spectral fluorescence imaging was performed again after PDT.

Photodynamic therapy

Both continuous and pulsed irradiation modes were used for PDT. The laser LFT-02-BIOSPEC (BIOSPEC Ltd., Moscow) with a 635 nm wavelength and the maximum output power of 1.5 W was used in continuous irradiation mode. Laser radiation delivery was carried out through a quartz optical fiber with a polymer shell with a total

**Рис. 6.** Общая схема проведения исследования.
Fig. 6. General scheme of the study.

diameter of 600 μm . Output power of laser emission was varied in the range of 400-1200 mW.

Skin neoplasms were continuously irradiated with a wavelength 635 nm and a power density of 380-440 mW/cm². The energy dose was 95-100 J/cm². Laser irradiation was stopped when the pain effect increased. A significant increase in pain symptoms exceeding the pain threshold was recorded 10-20 sec after the beginning of continuous irradiation. After this, laser irradiation in pulse mode was performed. Pulsed irradiation of pathologic tissues with PpIX accumulation contributes to the pain reduction of patients in the light exposure area [5]. To minimize the impact on the surrounding healthy tissues, a medical dressing with a 10 mm hole diameter was applied to the pathological tissues area before pulse irradiation. A pulse system based on a ring xenon gas discharge lamp (BIOSPEC Ltd., Moscow) was used for pulsed PDT treatment. Patients received 10-12 pulses sequentially with an average energy density of 1 J/cm² and a total energy dose of 10-12 J/cm². Applying the pulse mode allowed to reduce pain in patients during PDT of tissues with PpIX accumulation.

Results and discussion

The spectral fluorescence study was performed with fluorescence excitation at wavelengths of 405 and 632.8 nm. This approach allowed the diagnosis of both superficial and deeper tissue layers [6]. Fig. 7 shows the spectral data of PpIX accumulation under fluorescence excitation at wavelengths $\lambda_{\text{exc}} = 405$ nm and $\lambda_{\text{exc}} = 632.8$ nm. The recorded data include diffusely scattered laser

irradiation and fluorescence of tissue from a patient with a dermatofibroma: central region and tumor periphery.

When fluorescence was excited at $\lambda_{\text{exc}} = 405$ nm, two intense peaks were recorded at 625-670 nm and 700-740 nm. A fluorescence peak in the 690-740 nm wavelength region was observed by irradiation at $\lambda_{\text{exc}} = 632.8$ nm. Fig. 8 shows the integral fluorescence intensities distribution in the indicated spectral ranges.

The results show that during the 4-hour observation period after the application of 5-ALA, an increase in the accumulation of PpIX was observed both in the superficial (Fig. 8a, b) and in the deeper (Fig. 8c) tissue layers. PDT was performed in the zones of PpIX accumulation. After PDT, a new fluorescence peak was registered in the wavelength range of 670-700 nm under laser excitation at a wavelength of 405 nm (Fig. 9).

Earlier in [7] it was shown that laser irradiation with a wavelength of 635 nm and an energy dose of 43 J/cm² of human adenocarcinoma cells leads to the formation of photodynamically active PpIX photoproducts. These photoproducts that fluoresce with a minor short-wavelength shift, are characterized as a mixture of chlorin-type photoproducts [7]. The main photoproduct in the mixture is photoporphyrin: two chlorin-type hydroxyaldehyde isomers that exhibit fluorescence in the wavelength range of 670-690 nm.

Chlorin-type photoproducts differ from PpIX by the presence of an absorption band in the 450 nm region and an intense fluorescence peak in the 650-700 nm wavelength range. The property of PpIX photoproducts

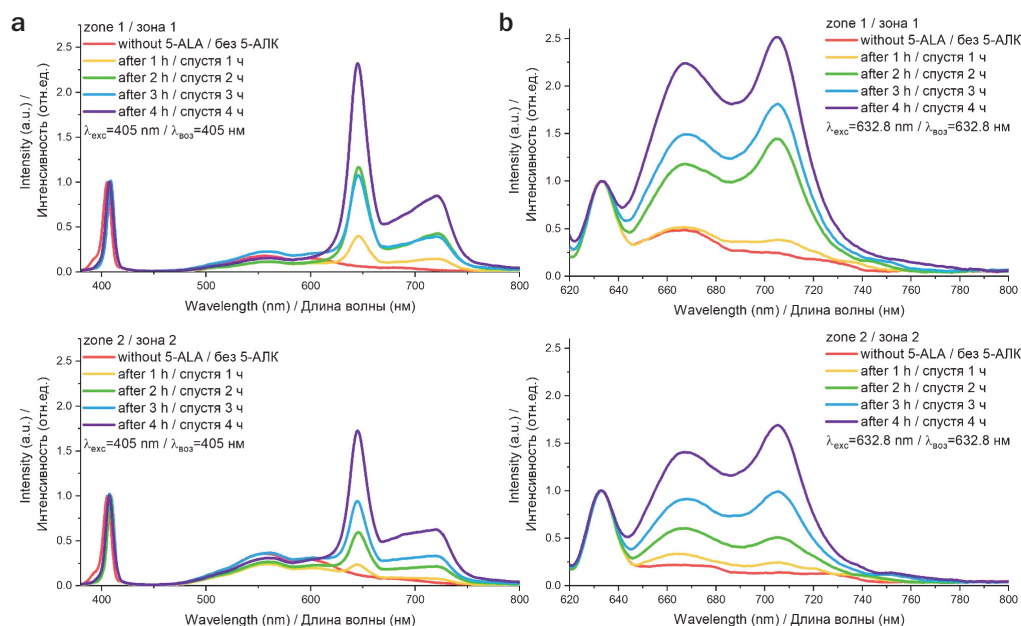


Рис. 7. Спектральные данные, включающие диффузно рассеянное лазерное излучение и флуоресценцию в центральной области (зона 1) и периферии (зона 2) дерматофибромы в различные временные точки после введения 5-АЛК: (а) при $\lambda_{\text{exc}} = 405$ nm; (б) при $\lambda_{\text{exc}} = 632.8$ nm. Спектры нормированы на максимальное значение интенсивности диффузно рассеянного лазерного излучения.

Fig. 7. Spectral data including diffusely scattered laser radiation and fluorescence in the central area (zone 1) and periphery (zone 2) of dermatofibroma at different time points after 5-ALA administration: (a) at $\lambda_{\text{exc}} = 405$ nm; (b) at $\lambda_{\text{exc}} = 632.8$ nm. The spectra were normalized to the maximum intensity of diffusely scattered laser radiation.

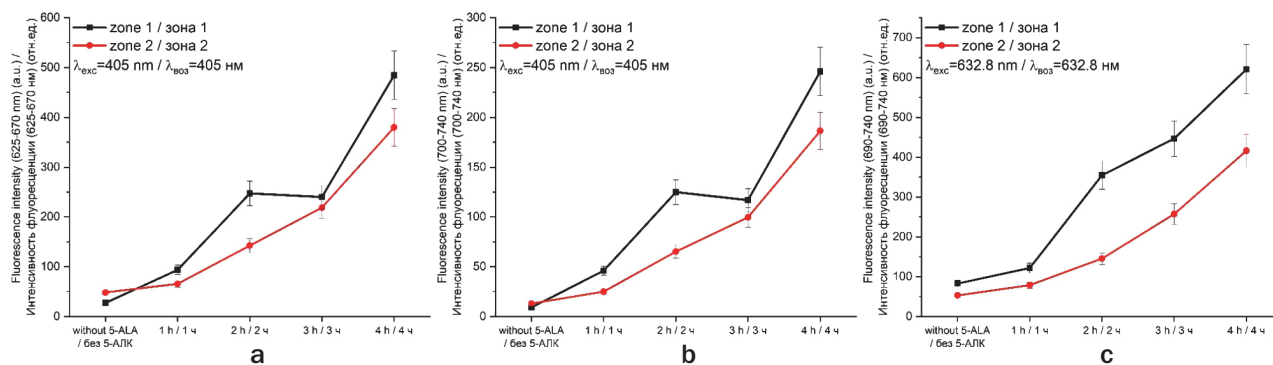


Рис. 8. Распределение интегральных интенсивностей флуоресценции в центральной области (зона 1) и периферии (зона 2) дерматофибром: а – в диапазоне 625-670 нм; б – в диапазоне 700-740 нм; с – в диапазоне 690-740 нм.

Fig. 8. Distribution of integrated fluorescence intensities in the central region (zone 1) and periphery (zone 2) of dermatofibroma: а – in the range of 625-670 nm; б – in the range of 700-740 nm; с – in the range of 690-740 nm.

is sometimes used to improve the efficiency and contrast of 5-ALA fluorescence navigation [8]. Exposure to 635 nm laser excitation leads to a decrease in the PpIX fluorescence intensity and is followed by the formation of a new fluorescence peak at 675 nm [8].

An increase in tissue fluorescence intensity in the 670-700 nm wavelength range was also recorded in both central and peripheral regions of dermatofibroma, indicating the presence of chlorin-type photoproducts in tissue after PDT. PpIX photoproducts have photodynamic activity and can be used in 5-ALA-PDT. The quantum yield of singlet oxygen of photoporphyrin is 0.69 [9].

To evaluate the contribution of photoproduct fluorescence to the recorded signal, the photoporphyrin

fluorescence index was calculated as the ratio of the integral fluorescence intensities in the 670-700 nm wavelength range to the integral intensity in the 625-670 nm wavelength range (Fig. 10).

Currently, scattered data are available on the dynamics of 5-ALA-induced PpIX accumulation. The maximal accumulation time of PpIX may vary depending on the route of administration of 5-ALA as well as the tumor type. The most common 5-ALA-PDT of skin tumors is performed by topical (local) drug administration in the form of gel or aqueous solution. This route of administration demonstrates a more rapid PpIX accumulation in tissues compared to oral and inhalation administration of 5-ALA [10]. The PpIX maximum accumulation in skin tumors is observed by 3.5-6

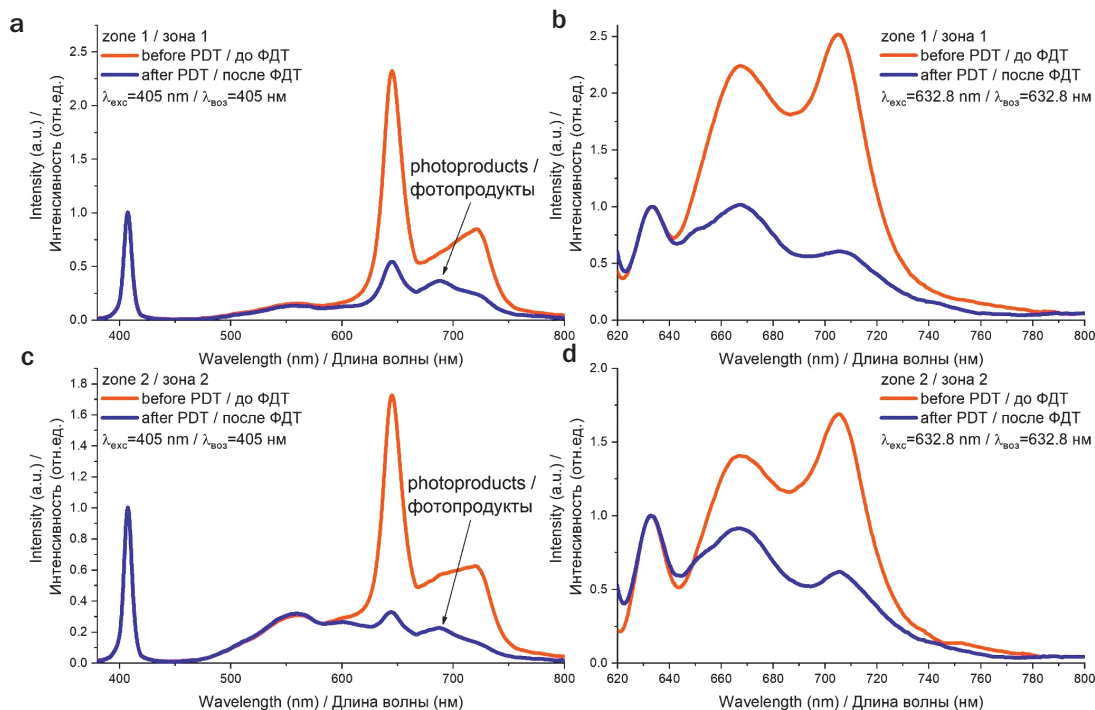


Рис. 9. Результаты спектрально-флуоресцентной диагностики в центральной области (зона 1) и периферии (зона 2) дерматофибром: а – до ФДТ (спустя 4 ч после введения 5-АЛК); б – после ФДТ.

Fig. 9. Results of spectral fluorescence diagnostics in the central area (zone 1) and periphery (zone 2) of dermatofibroma: а – before PDT (4 hours after 5-ALA administration); б – after PDT.

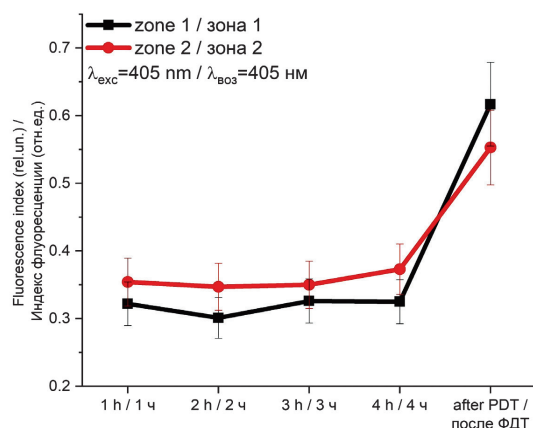


Рис. 10. Изменение флуоресценции фотопродуктов хлоринового типа в процессе накопления 5-АЛК-индуцированного ПпIX и после проведения ФДТ дерматофибромы ($\lambda=635$ нм, плотность мощности 380 мВт/см², доза энергии 100 Дж/см²).
Fig. 10. Changes in the fluorescence of chlorin-type photoproducts during the accumulation of 5-ALA-induced PpIX and after PDT ($\lambda=635$ nm, power density 380 mW/cm², energy dose 100 J/cm²).

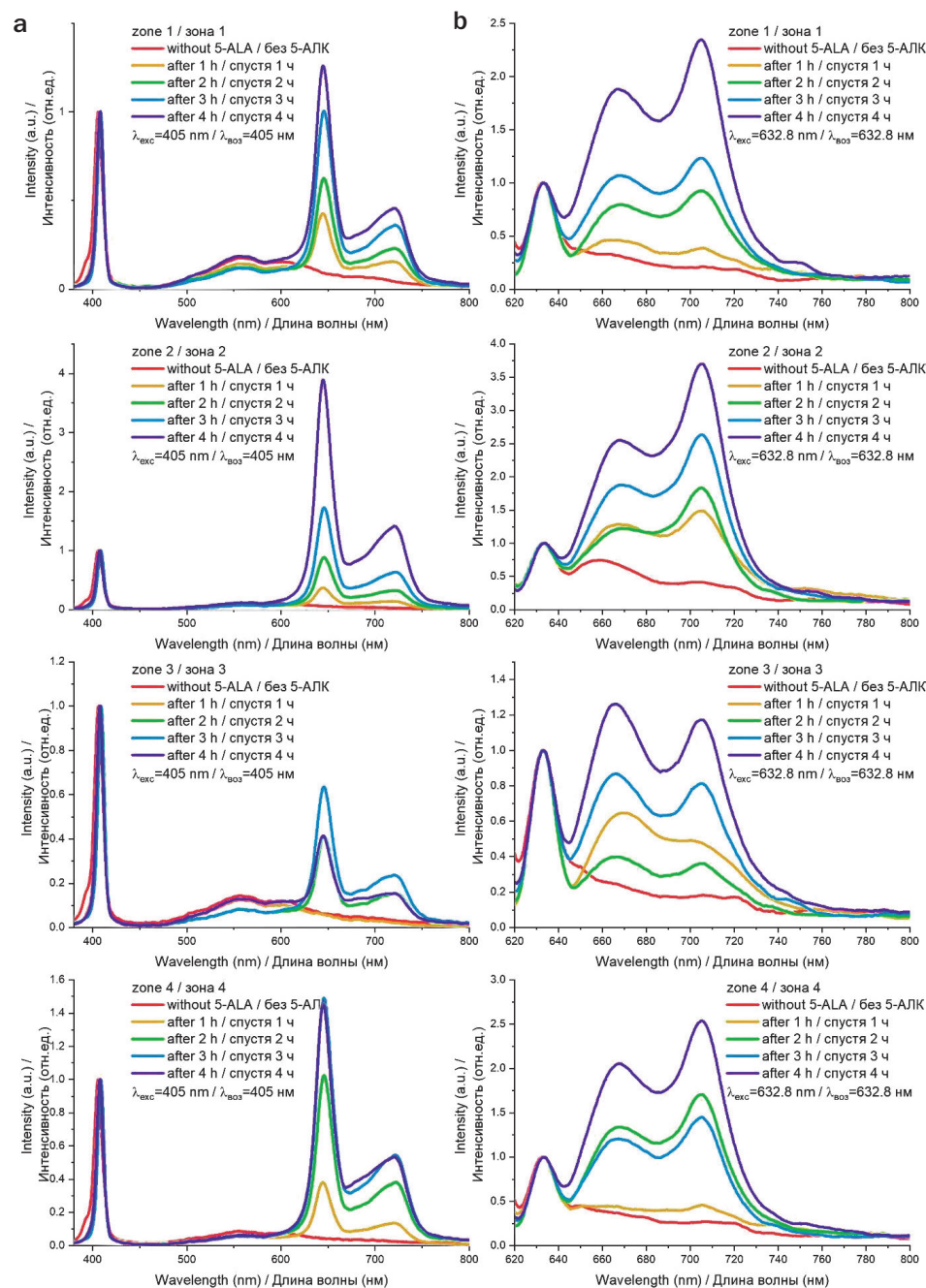


Рис. 11. Спектральные данные, включающие диффузно рассеянное лазерное излучение и флуоресценцию тканей меланоцитарного невуса в зонах с повышенным содержанием меланоцитов (зоны 1-3) и в зоне, относительно свободной от меланоцитов (зона 4): а – при $\lambda_{\text{вoз}}=405$ нм; б – при $\lambda_{\text{вoз}}=632,8$ нм. Спектры нормированы на максимальное значение интенсивности диффузно рассеянного лазерного излучения.
Fig. 11. Spectral data including diffusely scattered laser radiation and fluorescence of melanocytic nevus tissues in areas with an increased content of melanocytes (zones 1-3) and in an area relatively free of melanocytes (zone 4): а – at $\lambda=405$ nm; б – at $\lambda=632.8$ nm.

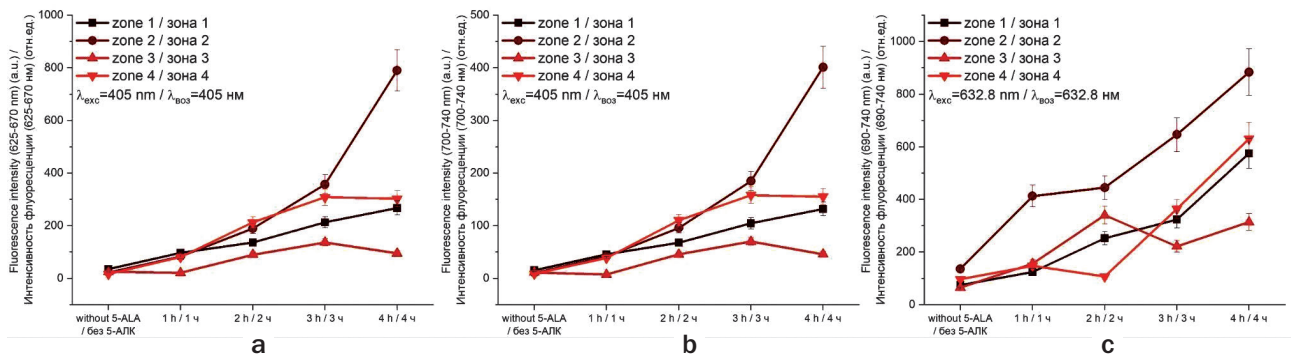


Рис. 12. Распределение интегральных интенсивностей флуоресценции тканей меланоцитарного невуса в зонах с повышенным содержанием меланоцитов (зоны 1-3) и в зоне, относительно свободной от меланоцитов (зона 4): а – в диапазоне 625-670 нм; б – в диапазоне 700-740 нм; с – в диапазоне 690-740 нм.

Fig. 12. Distribution of integrated fluorescence intensities of melanocytic nevus tissues in areas with an increased content of melanocytes (zones 1-3) and in an area relatively free of melanocytes (zone 4): а – in the range of 625-670 nm; б – in the range of 700-740 nm; с – in the range of 690-740 nm.

h after application of 5-ALA [11]. For example, in squamous cell cancer with local injection of a 20% solution of 5-ALA, peak accumulation was recorded after 4 h, whereas in basal cell cancer it was recorded 6 h after administration [11].

In case of the patient with congenital melanocytic nevus, intensive PpIX accumulation was registered as early as 1 h after 5-ALA application, both in the areas

with increased melanocyte content (zones 1-3) and in the area relatively free of melanocytes (zone 4) (Fig. 11).

The spectra were normalized to the maximum value of the intensity of diffusely scattered laser radiation.

As in the case of the dermatofibroma patient, two intense peaks were recorded at $\lambda_{\text{exc}} = 405$ nm in the wavelength range of 625-670 nm and 700-740 nm. A

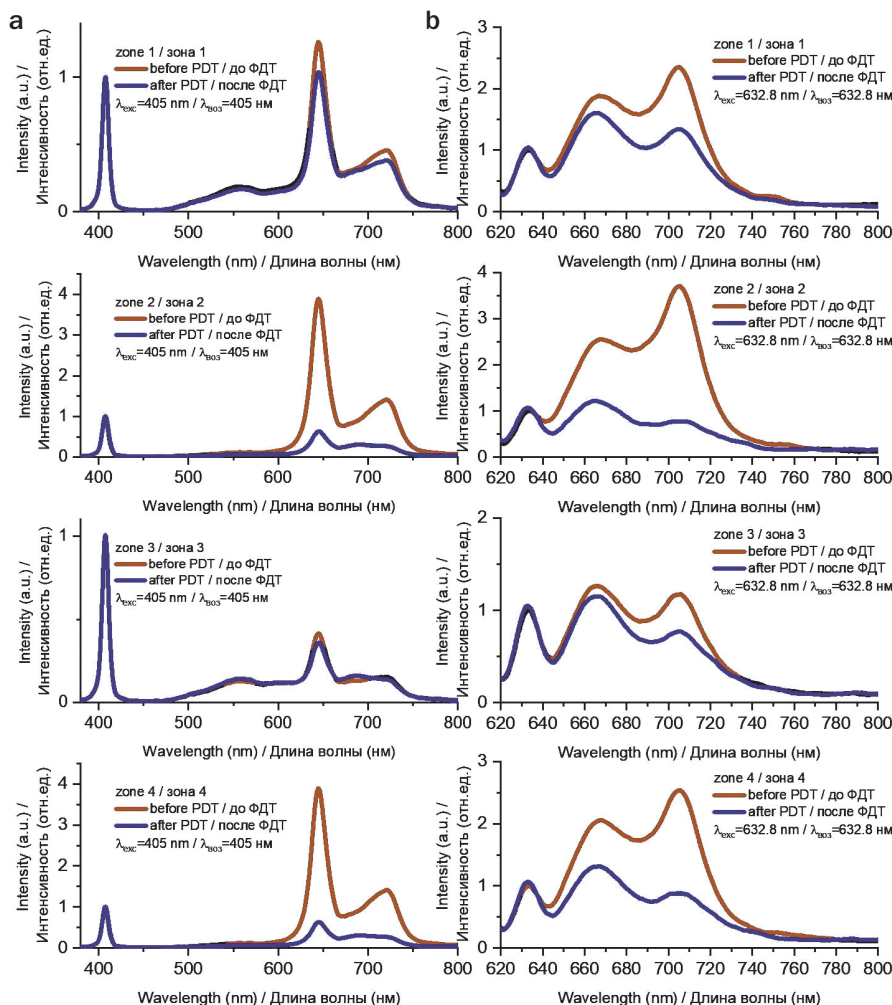


Рис. 13. Результаты спектрально-флуоресцентной диагностики меланоцитарного невуса в зонах с повышенным содержанием меланоцитов (зоны 1-3) и в зоне, относительно свободной от меланоцитов (зона 4): а – до ФДТ (спустя 4 ч после введения 5-АЛК); б – после ФДТ.

Fig. 13. Results of spectral fluorescence diagnostics of melanocytic nevus in areas with an increased content of melanocytes (zones 1-3) and in an area relatively free of melanocytes (zone 4): а – before PDT (4 h after 5-ALA administration); б – after PDT.

fluorescence peak in the region of 690-740 nm was observed at $\lambda_{\text{exc}} = 632.8$ nm. Fig. 12 shows the distribution of integrated fluorescence intensities in the indicated ranges.

In comparison to dermatofibroma tissues, the results showed that in the superficial tissue layers (at $\lambda_{\text{exc}} = 405$ nm) of the investigated zones 3 and 4, the PpIX maximum accumulation was observed 3 h after 5-ALA application (Fig. 12a,b). The 5-ALA-induced PpIX accumulation continued to increase 4 h after injection (Fig. 12c) in deeper tissue layers (at $\lambda_{\text{exc}} = 632.8$ nm). PDT was performed in all areas. Photobleaching of PpIX was observed in both superficial and deeper tissue layers as a result (Fig.13).

Photoporphyrin formation was observed in all investigated areas of melanocytic nevus after PDT (Fig. 14). There was no correlation between the intensity of photoporphyrin formation and the intensity of PpIX accumulation (Fig. 12, 14).

PpIX photoproducts are of great interest and offer new opportunities for high-contrast fluorescence imaging using 5-ALA [8]. PpIX photoproducts can easily move in the intracellular space due to their greater water solubility compared to PpIX [12], and be less sensitive to the singlet oxygen generated by PpIX [13]. Despite the lower singlet oxygen generation efficiency compared to PpIX, PpIX photoproducts can potentially be used for PDT [7, 14]. In summary, PpIX photoproducts can expand the fluorescence diagnostic capabilities and improve the efficiency of PDT, which requires further research for their practical application.

Conclusion

The dynamics of PpIX accumulation in superficial and deep dermatofibroma layers and congenital melanocytic nevus with fluorescence excitation at wavelengths 405

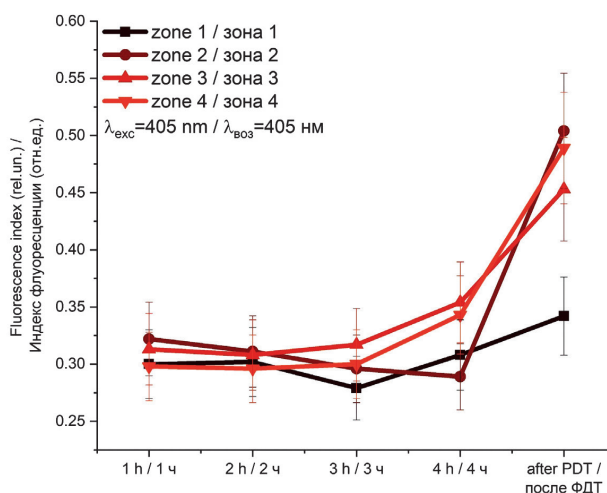


Рис. 14. Изменение флуоресценции фотопродуктов хлоринового типа в процессе накопления 5-АЛК-индуцированного ПпИХ и после проведения ФДТ меланоцитарного невуса ($\lambda = 635$ nm, плотность мощности 380 мВт/см², доза энергии 100 Дж/см²).

Fig. 14. Changes in fluorescence of chlorin-type photoproducts during the accumulation of 5-ALA-induced PpIX and after PDT of melanocytic nevus ($\lambda = 635$ nm, power density 380 mW/cm², energy dose 100 J/cm²).

and 632.8 nm with administration of a 20% 5-ALA solution was studied. PpIX accumulation in dermatofibroma tissues continued to increase during 4 h of observation in both superficial and deep tissue layers, in the central and the peripheral regions of the tumor. In comparison to melanocytic nevus tissues, maximum PpIX accumulation in superficial layers was reached after 3 h, while in deep layers an increase in PpIX accumulation within 4 h was observed. It is found that in the process of tumor PDT by laser excitation with a 635 nm wavelength, chlorin-type photoproducts characterized by intense fluorescence in the range of 670-700 nm are formed.

REFERENCES

- Beika M., Harada Y., Minamikawa T., Yamaoka Y., Koizumi N., Murayama Y., Konishi H., Shiozaki A., Fujiwara H., Otsuji E., Takamatsu T. and Tanaka H. Accumulation of Uroporphyrin I in Necrotic Tissues of Squamous Cell Carcinoma after Administration of 5-Aminolevulinic Acid. *International Journal of Molecular Sciences*, 2021, Vol. 22(18), pp. 10121. <https://doi.org/10.3390/ijms221810121>
- Du H., Amy Fuh R., Li J., Corkan L.A. and S. Lindsey J. PhotochemCAD: A computer-aided design and research tool in photochemistry. *Photochemistry and Photobiology*, 1998, Vol. 68, pp.141-142. <https://doi.org/10.1111/j.1751-1097.1998.tb02480.x>
- Dixon J. M., Taniguchi M. and S. Lindsey J. PhotochemCAD 2. A refined program with accompanying spectral databases for photochemical calculations. *Photochemistry and Photobiology*, 2004, Vol. 81, pp. 212-213. <https://doi.org/10.1111/j.1751-1097.2005.tb01544.x>
- Khilov, Aleksandr Vladimirovich, et al. "Analytical model of fluorescence intensity for the estimation of fluorophore localisation in biotissue with dual-wavelength fluorescence imaging" *Quantum Electronics*, 2021, Vol. 51(2), pp. 95. DOI 10.1070/QEL17503

ЛИТЕРАТУРА

- Beika M., Harada Y., Minamikawa T., Yamaoka Y., Koizumi N., Murayama Y., Konishi H., Shiozaki A., Fujiwara H., Otsuji E., Takamatsu T. and Tanaka H. Accumulation of Uroporphyrin I in Necrotic Tissues of Squamous Cell Carcinoma after Administration of 5-Aminolevulinic Acid // *International Journal of Molecular Sciences*. – 2021. – Vol. 22(18).– P. 10121. <https://doi.org/10.3390/ijms221810121>
- Du H., Amy Fuh R., Li J., Corkan L.A. and S. Lindsey J. PhotochemCAD: A computer-aided design and research tool in photochemistry // *Photochemistry and Photobiology*. – 1998. – Vol. 68. – P.141-142. <https://doi.org/10.1111/j.1751-1097.1998.tb02480.x>
- Dixon J. M., Taniguchi M. and S. Lindsey J. PhotochemCAD 2. A refined program with accompanying spectral databases for photochemical calculations // *Photochemistry and Photobiology*. – 2004. – Vol. 81. – P.212-213. <https://doi.org/10.1111/j.1751-1097.2005.tb01544.x>
- Khilov, Aleksandr Vladimirovich, et al. "Analytical model of fluorescence intensity for the estimation of fluorophore localisation in biotissue with dual-wavelength fluorescence imaging" // *Quantum Electronics*. – 2021. – Vol. 51(2). – P. 95. DOI 10.1070/QEL17503

5. Efendiev K., Alekseeva P.M., Bikmukhametova I.R., Piteriskova L.S., Orudzhova K.F., Agabekova U.D., Slovokhodov E.K. and Loschenov V.B. Comparative investigation of 5-aminolevulinic acid and hexyl aminolevulinate-mediated photodynamic diagnostics and therapy of cervical dysplasia and vulvar leukoplakia. *Laser Physics Letters*, 2021, Vol. 18(6), pp. 065601. DOI 10.1088/1612-202X/abf5cf
6. Kirillin, M., Khilov, A., Kurakina, D., Orlova, A., Perekatova, V., Shishkova, V., ... & Sergeeva, E. (2021). Dual-wavelength fluorescence monitoring of photodynamic therapy: from analytical models to clinical studies. *Cancers*, 13(22), pp. 5807. <https://doi.org/10.3390/cancers13225807>
7. Bagdonas S., Ma L.W., Iani V., Rotomskis R., Juzenas P. and Moan J. Phototransformations of 5-Aminolevulinic Acid-induced Protoporphyrin IX in vitro: A Spectroscopic Study. *Photochemistry and photobiology*, 2000, Vol. 72(2), pp. 186-192. [https://doi.org/10.1562/0031-8655\(2000\)0720186POAAIP2.0.CO2](https://doi.org/10.1562/0031-8655(2000)0720186POAAIP2.0.CO2)
8. Ogbonna Sochi J., Y. York W.B., Nishimura T., Hazama H., Fukuhara H., Inoue K. and Awazu K. Increased fluorescence observation intensity during the photodynamic diagnosis of deeply located tumors by fluorescence photoswitching of protoporphyrin IX. *Journal of Biomedical Optics*, 2023, pp. 055001-055001. <https://doi.org/10.1117/1.JBO.28.5.055001>
9. Sidney Cox G., Bobillier C. and G. Whitten D. Photooxygenation and singlet oxygen sensitization by protoporphyrin IX and its photooxygenation products. *Photochemistry and Photobiology*, 1982, Vol. 36, pp. 401-407. <https://doi.org/10.1111/j.1751-1097.1982.tb04393.x>
10. Rick K., Sroka R., Stepp H., Kriegmair M., Huber R.M, Jacob K. and Baumgartner R. Phototransformations of 5-Aminolevulinic Pharmacokinetics of Saminolevulinic acid-induced protoporphyrin IX in skin and blood. *Journal of Photochemistry and Photobiology: Biology*, 1997, Vol. 40, pp. 313-319. [https://doi.org/10.1016/S1011-1344\(97\)00076-6](https://doi.org/10.1016/S1011-1344(97)00076-6)
11. Fritsch C., Lehmann P., Stahl W., Schulte K.W., Blohm E., Lang K., Sies H. and Ruzicka T. Optimum porphyrin accumulation in epithelial skin tumours and psoriatic lesions after topical application of δ -aminolaevulinic acid. *British Journal of Cancer*, 1999, Vol. 79, pp. 1603-1608. <https://doi.org/10.1038/sj.bjc.6690255>
12. Brault D., Aveline B., Delgado O. and Vever-Bizet Ch. Chlorin-type photosensitizers derived from vinyl porphyrins. *Photochemistry and Photobiology*, 2001, Vol. 73(4), pp. 331-338. <https://doi.org/10.1117/12.199160>
13. Robinson D. J., de Bruijn H. S., van der Veen N., Stringer M. R., Brown S. B. and Star W. M. Fluorescence photobleaching of ALA-induced PpIX during photodynamic therapy of normal hairless mouse skin: the effect of light dose and irradiance and the resulting biological effect. *Photochemistry and Photobiology*, 1998, Vol. 67, pp. 140-149. <https://doi.org/10.1111/j.1751-1097.1998.tb05177.x>
14. Ogbonna, Sochi J., Katsuyoshi Masuda, and Hisanao Hazama. "The effect of fluence rate and wavelength on the formation of protoporphyrin IX photoproducts. " *Photochemical & Photobiological Sciences*, 2024, Vol. 23(9), pp.1627-1639. <https://doi.org/10.1007/s43630-024-00611-9>
5. Efendiev K., Alekseeva P.M., Bikmukhametova I.R., Piteriskova L.S., Orudzhova K.F., Agabekova U.D., Slovokhodov E.K. and Loschenov V.B. Comparative investigation of 5-aminolevulinic acid and hexyl aminolevulinate-mediated photodynamic diagnostics and therapy of cervical dysplasia and vulvar leukoplakia // *Laser Physics Letters*. – 2021. – Vol. 18(6) . – P.065601. DOI 10.1088/1612-202X/abf5cf
6. Kirillin, M., Khilov, A., Kurakina, D., Orlova, A., Perekatova, V., Shishkova, V., ... & Sergeeva, E. (2021). Dual-wavelength fluorescence monitoring of photodynamic therapy: from analytical models to clinical studies // *Cancers*. – 13(22). – P. 5807. <https://doi.org/10.3390/cancers13225807>
7. Bagdonas S., Ma L.W., Iani V., Rotomskis R., Juzenas P. and Moan J. Phototransformations of 5-Aminolevulinic Acid-induced Protoporphyrin IX in vitro: A Spectroscopic Study // *Photochemistry and photobiology*. – 2000. – Vol. 72(2). – P. 186-192. [https://doi.org/10.1562/0031-8655\(2000\)0720186POAAIP2.0.CO2](https://doi.org/10.1562/0031-8655(2000)0720186POAAIP2.0.CO2)
8. Ogbonna Sochi J., Y. York W.B., Nishimura T., Hazama H., Fukuhara H., Inoue K. and Awazu K. Increased fluorescence observation intensity during the photodynamic diagnosis of deeply located tumors by fluorescence photoswitching of protoporphyrin IX // *Journal of Biomedical Optics*. – 2023. – P. 055001-055001. <https://doi.org/10.1117/1.JBO.28.5.055001>
9. Sidney Cox G., Bobillier C. and G. Whitten D. Photooxygenation and singlet oxygen sensitization by protoporphyrin IX and its photooxygenation products // *Photochemistry and Photobiology*. – 1982. – Vol. 36. – P. 401-407. <https://doi.org/10.1111/j.1751-1097.1982.tb04393.x>
10. Rick K., Sroka R., Stepp H., Kriegmair M., Huber R.M, Jacob K. and Baumgartner R. Phototransformations of 5-Aminolevulinic Pharmacokinetics of Saminolevulinic acid-induced protoporphyrin IX in skin and blood // *Journal of Photochemistry and Photobiology: Biology*. – 1997. – Vol. 40. – P. 313-319. [https://doi.org/10.1016/S1011-1344\(97\)00076-6](https://doi.org/10.1016/S1011-1344(97)00076-6)
11. Fritsch C., Lehmann P., Stahl W., Schulte K.W., Blohm E., Lang K., Sies H. and Ruzicka T. Optimum porphyrin accumulation in epithelial skin tumours and psoriatic lesions after topical application of δ -aminolaevulinic acid // *British Journal of Cancer*. – 1999. – Vol. 79. – P. 1603-1608. <https://doi.org/10.1038/sj.bjc.6690255>
12. Brault D., Aveline B., Delgado O. and Vever-Bizet Ch. Chlorin-type photosensitizers derived from vinyl porphyrins // *Photochemistry and Photobiology*. – 2001. – Vol. 73(4) . – P. 331-338. <https://doi.org/10.1117/12.199160>
13. Robinson D. J., de Bruijn H. S., van der Veen N., Stringer M. R., Brown S. B. and Star W. M. Fluorescence photobleaching of ALA-induced PpIX during photodynamic therapy of normal hairless mouse skin: the effect of light dose and irradiance and the resulting biological effect // *Photochemistry and Photobiology*. – 1998. – Vol. 67. – P. 140-149. <https://doi.org/10.1111/j.1751-1097.1998.tb05177.x>
14. Ogbonna, Sochi J., Katsuyoshi Masuda, and Hisanao Hazama. "The effect of fluence rate and wavelength on the formation of protoporphyrin IX photoproducts. // " *Photochemical & Photobiological Sciences*. – 2024. – Vol. 23.9 – P.1627-1639. <https://doi.org/10.1007/s43630-024-00611-9>